

Vaccinia virus strain Western Reserve protein B14 is an intracellular virulence factor

Ron A.-J. Chen, Nathalie Jacobs and Geoffrey L. Smith

Department of Virology, Faculty of Medicine, Imperial College London, St Mary's Campus,
Norfolk Place, London W2 1PG, UK

Correspondence

Geoffrey L. Smith
glsmith@imperial.ac.uk

Supplementary figures showing analysis of recombinant VACV genomes, growth kinetics of v Δ B14 and the affect of virus virulence in a murine intranasal model are available as supplementary material in JGV Online.

A characterization of the *B14R* gene from *Vaccinia virus* (VACV) strain Western Reserve (WR) is presented. Computational analyses of the *B14R* gene indicated high conservation in orthopoxviruses but no orthologues outside the *Poxviridae*. To characterize the B14 protein, the *B14R* gene was expressed in *Escherichia coli* and recombinant protein was purified and used to generate a rabbit polyclonal antiserum. This antiserum recognized a 15 kDa cytoplasmic protein in mammalian cells that were transfected with the *B14R* gene or infected with VACV WR, but not from cells infected with a VACV mutant ($v\Delta B14$) from which the *B14R* gene was deleted. Compared to wild-type and revertant virus controls, $v\Delta B14$ had normal growth kinetics in cell culture. The virulence of $v\Delta B14$ was assessed in two *in vivo* models. Mice infected intranasally with $v\Delta B14$ had similar weight loss compared to the controls, but in C57BL/6 mice infected intradermally $v\Delta B14$ induced a smaller lesion size compared with controls. Moreover, intradermal infection with $v\Delta B14$ caused an increased infiltration of cells into the infected lesion despite the smaller lesion size. Therefore, B14 is an intracellular protein that is non-essential for virus replication in cell culture but contributes to virus virulence *in vivo* and affects the host response to infection.

INTRODUCTION

Vaccinia virus (VACV) is a member of the genus *Orthopoxvirus* of the *Poxviridae*, a family of large, dsDNA viruses replicating in the cytoplasm (Moss, 2001). The VACV strain Copenhagen genome (191 kb) was predicted to encode around 200 genes (Goebel *et al.*, 1990) and the central region of the genome (~100 kb), like that of other chordopoxviruses, is highly conserved and contains 90 genes that are present in all sequenced chordopoxviruses (Upton *et al.*, 2003; Gubser *et al.*, 2004). Most of these genes encode proteins with essential functions for virus replication. In contrast, genes located in the terminal regions are more variable and encode proteins that are non-essential for virus replication but which affect virus virulence, host range and modulation of the host response to infection (Smith & McFadden, 2002). Immunomodulators from VACV and other poxviruses may act inside or outside the infected cell and may block the action of cytokines, chemokines and interferons, or intracellular signalling pathways leading to apoptosis or gene activation (Seet *et al.*, 2003).

The *B14R* gene of VACV strain Western Reserve (WR) is located in the right terminal region that is rich in immunomodulators. For instance, the upstream gene encodes an intracellular protein that inhibits caspase-1 activity and thereby induction of apoptosis (Dobbelstein & Shenk, 1996; Kettle *et al.*, 1997) and the downstream gene encodes a soluble interleukin (IL)-1 β -binding protein (Alcami & Smith, 1992; Spriggs *et al.*, 1992) that inhibits development of fever during systemic infection (Alcami & Smith, 1996). VACV strain WR *B14R* gene is predicted to encode a 149 aa protein (Howard *et al.*, 1991; Smith *et al.*, 1991). The equivalent gene in VACV strain Copenhagen is called *B15R* due to disruption of the preceding open reading frame (ORF) into fragments called *B13R* and *B14R* (Goebel *et al.*, 1990). Unusually for a gene located in a terminal region of the genome, VACV WR *B14R* gene is highly conserved among different orthopoxviruses, suggesting an important function (Gubser & Smith, 2002; Gubser *et al.*, 2004). Although the *B14R* gene is conserved, hitherto there has been no characterization of the encoded protein or functional analysis with viruses lacking this gene. We selected the *B14R* gene for study as part of our ongoing interest in VACV immunomodulatory proteins because of its location and conservation.

In this study, we identified the B14 protein in infected cells using specific antiserum, and constructed a VACV mutant lacking the *B14R* gene (v Δ B14) and a revertant in which the gene was reinserted into the deletion mutant (vB14-rev). The mutant virus was compared *in vitro* and *in vivo* to the wild-type (vB14) and revertant (vB14-rev) controls. Data presented show that although B14 is non-essential for virus replication in cell culture, it promotes VACV virulence in a murine intradermal (i.d.) model (Tschärke & Smith, 1999; Tschärke *et al.*, 2002; Reading & Smith, 2003) and influences the infiltration of cells into the infected lesion. As such, it represents another intracellular virulence factor that is also an immunomodulator. Its mechanism of action is under investigation.

METHODS

Cell culture. Rabbit kidney RK₁₃ cells, African green monkey kidney cells BS-C-1 and CV-1 cells were grown in Dulbecco's modified Eagle's medium (DMEM) supplemented with 10 % heat-inactivated fetal bovine serum (FBS) (Harlan Sera-Lab), 50 IU penicillin (Gibco-BRL) ml⁻¹, 50 µg streptomycin (Gibco-BRL) ml⁻¹ and 2 mM L-glutamine (Gibco-BRL). HeLa cells were purchased from the European Collection of Cell Cultures.

Construction of plasmid vectors. Wild-type or modified *B14R* gene fragments were produced by PCR using VACV WR genomic DNA as template and were then cloned into pSJH7 (Hughes *et al.*, 1991) via *EcoRI* and *XbaI* restriction sites. To produce plasmid pΔB14, a DNA fragment containing the left and right flanking regions of the *B14R* gene but lacking the entire *B14R* ORF was produced by overlapping PCR. The 5' fragment was generated with oligonucleotides 5'-GGAATTCCTTCGGTTCAACTGGAGATTA-3' (L-FA), containing an *EcoRI* restriction site (underlined) and 5'-AAATGTCAAGATGTACAACCTTACCAATTGCAATTGGAA-3', containing nucleotides from the 3' fragment (italics) at the 5' end. The 3' fragment was generated with oligonucleotides 5'-GTTGTACATCTTGACATTT-3', complementary sequence to the 5' fragment and 5'-GCTCTAGAGCATTGCTACCATTATCTATC-3' (R-FB), containing an *XbaI* restriction site (underlined). Based on the overlapping region, these two fragments were joined by PCR using the L-FA and R-FB oligonucleotides to become an FA–FB fragment. To generate pB14-rev, a DNA fragment containing the entire *B14R* gene and flanking regions was generated with oligonucleotides FA and FB. To construct a C-terminal haemagglutinin (HA)-tagged B14 VACV (vB14-HA), two fragments were generated and then joined by overlapping PCR. The first fragment was produced by PCR with oligonucleotides L-FA and 5'-AACATCGTATGGGTACATATTCATACGCCGGAATATGA-3', encoding part of an HA peptide DNA sequence (italics). The second fragment was amplified by PCR with oligonucleotides R-FB and 5'-ATGTACCCATACGATGTTCCAGATTACGCTTGATGAGTTGTACATCTTGA-3', containing the entire HA peptide DNA sequence (italics). These two fragments were joined with the L-FA and R-FB to become pSJH7-B14-HA.

To express the wild-type B14 protein and B14 tagged at the C terminus with HA in mammalian cells, DNA fragments were generated by PCR using pSJH7-B14-HA as template. For wild-type B14 expression (pCI-B14), a DNA fragment containing the *B14R* gene was produced by PCR with oligonucleotides 5'-GGAATTCCATGACGGCCAACCTTTAGTACC-3' (L-B14), containing an *EcoRI* restriction site (underlined) and 5'-GCTCTAGAGCTCATCAATTCATACGCCGGA-3', containing an *XbaI* restriction site (underlined). For expression of C-terminal HA tagged B14 (pCI-B14-HA), a DNA fragment encoding the HA peptide fused to the 3' end of *B14R* gene was generated by PCR with oligonucleotides L-B14 and 5'-GCTCTAGAGCTCATCAAGCGTAATCTGGAAC-3', containing *XbaI* restriction site (underlined) and nucleotides for the HA peptide (italics). These two fragments were cloned into the pCI vector (Promega) by *EcoRI* and *XbaI* restriction sites to

become pCI-B14-HA. The fidelity of the PCR-derived regions from all plasmids was verified by DNA sequencing.

Construction of recombinant viruses. A VACV deletion mutant lacking the *B14R* gene coding sequences ($v\Delta B14$), a revertant virus with these sequences reintroduced ($vB14$ -rev) and a virus containing a *B14R* gene encoding a C-terminal HA-tag ($vB14$ -HA) were constructed. The modified and wild-type *B14R* gene were inserted into plasmid pSJH7 (Hughes *et al.*, 1991), containing the *E. coli* guanine xanthine phosphoribosyltransferase gene as a selectable marker (Boyle & Coupar, 1988). The plasmids were then transfected into either VACV WR-infected CV-1 cells (to make $v\Delta B14$) or $v\Delta B14$ -infected cells (to make $vB14$ -rev and $vB14$ -HA), and recombinant viruses were isolated by transient dominant selection (Falkner & Moss, 1990).

Immunoblotting. Transfected or infected cells were lysed and prepared for immunoblotting as described previously (Parkinson & Smith, 1994).

Immunofluorescence. Cells used for fluorescent and confocal microscopy were grown on sterilized glass coverslips (borosilicate glass; BDH) in six-well plates. The cells were washed three times in ice-cold PBS, fixed in 4 % paraformaldehyde in PBS for 1 h at room temperature and incubated with 0.1 % Triton X-100 (Sigma) for 10 min at room temperature. The samples were blocked with 10 % FBS in PBS for 1 h at room temperature (or 4 °C overnight), incubated with primary antibody (Ab) at room temperature for 1 h and washed three times in PBS. Samples were then incubated with fluorescein isothiocyanate- or tetramethylrhodamine isothiocyanate-conjugated secondary Ab at room temperature for 1 h, washed three times with PBS and mounted in Mowiol-4',6-diamidino-2-phenylindole medium. Samples were examined with a Zeiss 512 laser scanning confocal microscope and images were reconstructed and processed using Confocal Assistant and Adobe Photoshop software.

Virus growth curves. Monolayers of BS-C-1 or CV-1 cells were infected with either 10 or 0.01 p.f.u. per cell for measurement of one-step or multi-step growth kinetics, respectively. The culture supernatant was removed at the indicated times and centrifuged at 800 **g** at 4 °C for 10 min to collect detached cells. Attached cells were scraped into DMEM/2.5 % FBS, added to the cells collected from the supernatant, frozen and thawed three times and sonicated to obtain the cell-associated virus. Infectious virions were determined by plaque assay on duplicate BS-C-1 cell monolayers.

Virulence assays. For murine intranasal (i.n.) models, female BALB/c mice (5–6 weeks old) were anaesthetized and infected intranasally with the indicated viral dosage in 20 μ l PBS (Williamson *et al.*, 1990). For the murine i.d. model, female C57BL/6 mice (6–8 weeks old) were anaesthetized and injected intradermally in the left ear pinnae with either 10⁴ p.f.u. per 10 μ l PBS per ear as described previously (Tschärke & Smith, 1999).

Analysis of cell populations in infected ears by flow cytometry. At the indicated times, intradermally infected mice were sacrificed and ears were removed. The infiltrate was collected and analysed as described previously (Reading & Smith, 2003; Jacobs *et al.*, 2006). Briefly, cells in the i.d. compartment migrated into RPMI 1640 medium (Gibco-BRL) containing 50 IU penicillin (Gibco-BRL) ml^{-1} , 50 μg streptomycin (Gibco-BRL) ml^{-1} , 10 % FBS and 2.5 mM HEPES, pH 7.4 in a plastic plate. Adherent and non-adherent cells were pooled, washed once with RPMI/10 % FBS, once with Tris/ NH_4Cl buffer (0.14 M NH_4Cl in 17 mM Tris, pH 7.2) and twice with FC buffer (0.1 % BSA, 0.1 % NaN_3 in PBS). Dermal cells were identified by the staining of surface markers: CD3 [phycoerythrin (PE) anti-CD3; Becton Dickinson] on T lymphocytes, Ly6-G (PE anti-Ly6-G; Becton Dickinson) on neutrophils and F4/80 (tri-color-anti-F4/80; Caltag Laboratories) on macrophages.

Statistical analysis. Student's *t*-test (two tailed, unpaired) was used to examine the significance of raw data.

RESULTS

Computational analysis of the B14 protein

The VACV WR *B14R* gene (GenBank accession no. AAO89475) was predicted to encode a 17.3 kDa protein (Howard *et al.*, 1991; Smith *et al.*, 1991) without a transmembrane domain or a secretory signal peptide (see www.poxvirus.org). Computational comparisons detected no orthologues outside poxviruses but found very similar proteins predicted to be encoded by many orthopoxviruses including other VACV strains, *Variola virus*, *Camelpox virus*, *Monkeypox virus*, *Ectromelia virus* and *Cowpox virus* with 94–98 % amino acid identity. The phylogenetic relationships of these proteins are shown in a rooted tree (Fig. 1, group I) produced from the aligned amino acid sequences. Another group of more distantly related orthopoxvirus proteins, typified by protein B22 from VACV Copenhagen, was identified and had between 41 and 42 % amino acid identity and between 57 and 61 % amino acid similarity (Fig. 1, group II). In some other chordopoxvirus genera, e.g. *Yatapoxvirus*, *Capripoxvirus*, *Leporipoxvirus* and *Suipoxvirus*, there are proteins related to B14 that have between 30 and 41 % amino acid identity and between 49 and 63 % amino acid similarity (Fig. 1 group III). However, these proteins clustered more closely with group II proteins from orthopoxviruses than with B14 and the group I proteins. For additional analysis of this family of protein see www.poxvirus.org. The B14 family is part of Poxvirus A4/B15 family (PF06225) and, interestingly, proteins related to B14 are not found in the genera *Avipoxvirus* and *Molluscipoxvirus* (see www.sanger.ac.uk/Software/Pfam).

The generation of *B14R* mutant VACV-WR

To study the function of B14 protein in virus-infected cells several recombinant viruses were constructed based on VACV strain WR (Methods). These included a plaque-purified wild-type (vB14), deletion mutant (vΔB14), revertant (vB14-rev) and HA-tagged B14 (vB14-HA). The genomes of these viruses were analysed by PCR and restriction enzyme digestion using DNA extracted from purified intracellular mature virus (IMV) (see Supplementary Fig. S1 and S2 available in JGV Online). PCR using primers for the *B14R* gene locus confirmed the presence of the *B14R* gene in vB14, vB14-rev and vB14-HA and its absence in vΔB14 (Supplementary Fig. S1 available in JGV Online). Digestion of genomic DNA with *SphI* showed similar fragments for all viruses, except that a fragment of approximately 3 kb was reduced in size by 500 bp in vΔB14 compared with controls (Supplementary Fig. S2 available in JGV Online), consistent with the loss of the B14R coding sequences. Similar analysis with enzymes *HindIII* and *SaI* found no differences outside the *B14R* locus (data not shown).

Identification of B14 expression using polyclonal antiserum

To identify the B14 protein in mammalian cells, the *B14R* gene was expressed in *E. coli* with an N-terminal His-tag and the recombinant protein was purified by Ni²⁺-affinity column (data not shown) and used to raise a rabbit anti-B14 polyclonal Ab. Immunoblot analysis using this Ab identified a 15 kDa protein in extracts of cells transfected with a plasmid containing the B14R

ORF driven by the human cytomegalovirus immediate-early promoter (Fig. 2a) and in cells infected by VACV WR (Fig. 2b). The specificity of the Ab was confirmed by its recognition of the 15 kDa protein (i) only in cells transfected with the B14R ORF but not the empty vector, and (ii) in cells infected with wild-type and revertant viruses but not $v\Delta B14$ (Fig. 2b, lower panel). The protein was not detected in highly purified VACV IMV virions or in the tissue culture supernatant (data not shown). The B14 protein was also expressed in mammalian cells with an HA-tag fused to the C terminus. This protein was recognized by an anti-HA monoclonal antibody (mAb) and by the anti-B14 Ab, whereas the wild-type protein was recognized only by the latter (Fig. 2a). To determine the time of expression of B14 protein during VACV infection, cells were infected in the presence or absence of cytosine arabinoside (AraC), an inhibitor of viral DNA replication and late protein expression, and extracts of cells were prepared at different times post-infection (p.i.) and were then analysed by immunoblotting (Fig. 2c). B14 was detected from 2 h p.i., and at all times examined, and was present at higher levels at 8 h p.i. It was still detected in cells in the presence of AraC, indicating the protein was made during the early phase of infection. In contrast, AraC blocked the expression of D8, a protein known to be expressed late in the VACV life cycle (Niles & Seto, 1988).

The location of the B14 protein was examined in HeLa cells transfected with the plasmid encoding the HA-tagged B14 protein. Immunofluorescence analysis with the anti-HA mAb and anti-B14 Ab detected a diffuse cytoplasmic staining with no obvious co-localization to specific organelles or the cell surface and with relatively little staining in the nucleus (Fig. 3a, upper panels). Only a weak background signal was detected by pre-immune rabbit serum in the HA-tag-positive transfected cells (Fig. 3a, lower right panel). This indicated the specificity of anti-B14 Ab. To compare the location of B14 in transfected cells with those infected by VACV, at 8 h p.i. $vB14$ -infected cells were stained with the rabbit Ab and this detected a similar intracellular distribution (Fig. 3b, upper right panel). In $v\Delta B14$ -infected cells, the B14 Ab showed very little staining (Fig. 3b, lower right panel). The infection with both viruses was confirmed using a mAb against the VACV D8 protein that detects punctate cytoplasmic structures (Fig. 3b, left panels) that are virions as reported previously (van Eijl *et al.*, 2002; Carter *et al.*, 2003).

B14 is non-essential in cell culture

The role of B14 protein in the life cycle of VACV-WR was examined by characterizing the phenotype of $v\Delta B14$ in cell culture. The plaque size formed by $v\Delta B14$ was smaller than that formed by $vB14$ and $vB14$ -rev in CV-1 cells and slightly smaller in BS-C-1 but not in RK₁₃ cells (Fig. 4). The reduction in plaque size of CV-1 cells and BS-C-1 was 40 and 20 %, respectively ($n=20$ plaques; $P<0.05$, Student's *t*-test). To examine the effect of B14 on the viral life cycle in more detail *in vitro*, one-step (Fig. 5a) and multi-step (Fig. 5b) growth curves were studied in BS-C-1 and CV-1 cells (Supplementary Fig. S3 available in JGV Online). In both cell types $v\Delta B14$ showed similar growth kinetics to control viruses after high (10 p.f.u. per cell) or low multiplicity (0.01 p.f.u. per cell) of infection. Therefore, the basis for the cell type-specific plaque size reduction in BS-C-1 and CV-1 cells was not a reduced virus yield.

B14 affects virus virulence and the recruitment of leukocytes

The virulence of vΔB14 was compared to control viruses in two murine models. In an i.n. model, no significant difference in weight loss or signs of illness (data not shown) was observed in animals infected with vΔB14 at 10^4 or 3×10^3 p.f.u. compared to control viruses (see Supplementary Fig. S4 available in JGV Online). However, in an i.d. infection model, vΔB14 induced a significantly ($P < 0.05$) smaller lesion size from days 6 to 17 p.i. (Fig. 6a).

Measurement of infectious virus in infected lesions indicated that although the titres of infectious virus increased equally up to 2 days p.i., thereafter (days 5 and 7) titres were reduced in vΔB14-infected ear lobes compared with controls (Fig. 6b). These observations indicate that B14 enhances virus virulence, at least partly by restricting clearance of virus.

To start to address the mechanism by which B14 affects the outcome of infection *in vivo*, the cells in the infected ears were extracted, quantified by trypan blue exclusion and identified by flow cytometry (Methods). This revealed a statistically ($P < 0.05$) higher number of cells in vΔB14-infected ears at day 11 p.i. compared with tissue infected by control viruses (Fig. 7a). Interestingly, in vΔB14-infected cells at day 8 p.i., neutrophils represented a reduced percentage of the total cell population compared with controls (Fig. 7b), while the percentage of macrophages (Fig. 7c) and lymphocytes (Fig. 7d) were slightly higher than the controls. However, when the absolute number of each cell type was analysed, rather than the percentage of total cells, the number of macrophages (Fig. 7f) and T cells (Fig. 7g) were significantly higher in ears infected by vΔB14 than in ears infected by controls on day 8 p.i. By this criterion the number of neutrophils was not significantly different between the groups (Fig. 7e). In addition, CD4, CD8, T-cell receptor $\gamma\delta$ cells were also examined but showed no significant difference (data not shown). Therefore, the decrease in percentage of neutrophils on day 8 was likely to be attributable to the corresponding increase of macrophages and lymphocytes. A similar result was observed on day 5 p.i. when cells were extracted from ears by digestion with collagenase (Jacobs *et al.*, 2006) (data not shown).

DISCUSSION

This paper provides a characterization of the B14 protein of VACV strain WR that was uncharacterized hitherto. Data presented show that B14 is an intracellular, 15 kDa protein that is expressed early during infection and is non-essential for the viral life cycle. Loss of the B14 protein reduced virus virulence in a murine i.d. but not i.n. model. The attenuation was manifested by a decrease in lesion size, reduced virus titres and enhanced recruitment of macrophages and T cells. Collectively, this indicates that B14 is an intracellular immunomodulator.

In both infected and transfected cells B14 was predominantly cytoplasmic, indicating that other VACV proteins do not influence the location of this protein. Under the conditions examined, there was no apparent co-localization with specific organelles, although a weak nuclear staining was also apparent. Active nuclear import is dependent on a nuclear localization signal or carrier protein(s) such as importin that shuttle between the cytoplasm and nucleus. Alternatively, small proteins (less than 20–40 kDa) could pass through nuclear pores by passive diffusion (Macara, 2001; Xu & Massague, 2004). Therefore, the presence of some B14 in the nucleus might be via an unknown active transport system or simply by passive diffusion into the nucleus due to the small molecular mass of B14.

B14 is a non-essential protein based on *in vitro* characterization of $v\Delta B14$. Although the mutant displayed reduced plaque size compared with wild-type and revertant control viruses in BS-C-1 and CV-1 cells, the plaque formed by each virus was indistinguishable in size in RK₁₃ cells. However, $v\Delta B14$ failed to show a significant decrease in growth kinetics, even in BS-C-1 and CV-1 cells. The major factor determining plaque size is the ability to form virus-tipped actin tails beneath cell-associated enveloped virus particles at the cell surface that drive surface virions into surrounding cells, for review see Smith *et al.* (2002). However, an analysis of actin-tail formation in cells infected by $v\Delta B14$ showed no difference from controls (data not shown). Other VACV proteins affect the plaque size or morphology without inhibiting actin-tail formation. For instance, a VACV strain lacking kelch-like protein C2 produced plaques with a distinct morphology but the same size (Pires de Miranda *et al.*, 2003) and either the deletion (Parkinson *et al.*, 1995) or overexpression (Sanderson *et al.*, 1996) of the A38 protein reduced plaque size. Overall, B14 is not required for the virus replication and the basis for the restricted plaque size is not due to a cell-line-specific defect in viral growth or inability to form any actin tails.

In vivo analysis showed that B14 contributed to virus virulence in a murine i.d. (local infection) but not i.n. (systemic infection) model. Previously, other VACV immunomodulators were shown to exhibit a phenotype in either one model or the other and this may be explained by the different inflammatory responses following infection with VACV via the i.n. and i.d. routes (Tscharke *et al.*, 2002; Reading & Smith, 2003). Analysis of infectious virus titres in infected dermal tissue showed that by 2 days p.i. the virus titres had increased for all viruses to a similar extent; therefore, there was no replicative defect associated with loss of B14 *in vivo*. However, subsequently (days 5 and 7 p.i.) the titres of virus in ears infected with $v\Delta B14$ was reduced

compared with controls. This finding indicated that B14 impaired the ability of the host response to control virus growth, and so in its absence smaller lesions were produced.

To examine the effect of B14 *in vivo* further, cells that were present in the infected lesions were extracted and analysed by staining with specific mAb and FACS analysis. Although there was a trend showing an increased infiltration of cells into the v Δ B14-infected ears on days 5 and 8 p.i. this was only significantly different from controls at day 11 p.i. The absolute number of neutrophils present in infected lesions was not altered at any time point, but the number of macrophages and T cells rose significantly at day 8 p.i. in v Δ B14-infected lesions compared with controls. This increase in leukocytes indicates an enhanced host inflammatory response in the absence of B14, and may contribute to the size restriction and early resolution of the resulting lesion.

The recruitment of leukocytes to the skin is dependent on the expression of chemokines and cytokines (Gillitzer & Goebeler, 2001; Schon *et al.*, 2003). Among these mediators, chemokines CCL2 and CCL3 (formerly monocyte chemoattractant protein-1 and macrophage inflammatory protein-1 α , respectively) play important roles in recruiting T cells and macrophages (Kunstfeld *et al.*, 1998; von Stebut *et al.*, 2003). Therefore, the production of such chemokines early after infection will affect the cellular infiltrate. Infection by v Δ B14 caused a greater infiltrate in infected tissues on days 5–11 p.i. compared with infection by control viruses (although this was only significantly different on day 11). Notably these infiltrates contained increased numbers of T cells and macrophages (day 8 p.i.). Taken together, these findings suggest that B14 may modulate the inflammatory responses, possibly by affecting the expression of pro-inflammatory chemokines such as CCL2 and CCL3. However, the mechanism by which B14 exerts such immunomodulation remains to be investigated.

In summary, B14 is an intracellular virulence factor that is highly conserved in orthopoxviruses and modulates the host response to infection. These findings contribute to our understanding of poxvirus pathogenesis and suggest a means by which attenuated orthopoxvirus vaccines may be produced.

ACKNOWLEDGEMENTS

This work was supported by grants from the Wellcome Trust, the UK Medical Research Council and Imperial College London. R. A.-J. C. is the recipient of an Overseas Research Award scholarship and G. L. S. is a Wellcome Trust Principal Research Fellow.

REFERENCES

- Alcami, A. & Smith, G. L. (1992).** A soluble receptor for interleukin-1 β encoded by vaccinia virus: a novel mechanism of virus modulation of the host response to infection. *Cell* **71**, 153–167.
- Alcami, A. & Smith, G. L. (1996).** A mechanism for the inhibition of fever by a virus. *Proc Natl Acad Sci U S A* **93**, 11029–11034.
- Boyle, D. B. & Coupar, B. E. (1988).** A dominant selectable marker for the construction of recombinant poxviruses. *Gene* **65**, 123–128.
- Carter, G. C., Rodger, G., Murphy, B. J., Law, M., Krauss, O., Hollinshead, M. & Smith, G. L. (2003).** Vaccinia virus cores are transported on microtubules. *J Gen Virol* **84**, 2443–2458.
- Dobbelstein, M. & Shenk, T. (1996).** Protection against apoptosis by the vaccinia virus SPI-2 (B13R) gene product. *J Virol* **70**, 6479–6485.
- Falkner, F. G. & Moss, B. (1990).** Transient dominant selection of recombinant vaccinia viruses. *J Virol* **64**, 3108–3111.
- Gillitzer, R. & Goebeler, M. (2001).** Chemokines in cutaneous wound healing. *J Leukoc Biol* **69**, 513–521.
- Goebel, S. J., Johnson, G. P., Perkus, M. E., Davis, S. W., Winslow, J. P. & Paoletti, E. (1990).** The complete DNA sequence of vaccinia virus. *Virology* **179**, 247–266, 517–263.
- Gubser, C. & Smith, G. L. (2002).** The sequence of camelpox virus shows it is most closely related to variola virus, the cause of smallpox. *J Gen Virol* **83**, 855–872.
- Gubser, C., Hue, S., Kellam, P. & Smith, G. L. (2004).** Poxvirus genomes: a phylogenetic analysis. *J Gen Virol* **85**, 105–117.
- Howard, S. T., Chan, Y. S. & Smith, G. L. (1991).** Vaccinia virus homologues of the Shope fibroma virus inverted terminal repeat proteins and a discontinuous ORF related to the tumor necrosis factor receptor family. *Virology* **180**, 633–647.
- Hughes, S. J., Johnston, L. H., de Carlos, A. & Smith, G. L. (1991).** Vaccinia virus encodes an active thymidylate kinase that complements a *cdc8* mutant of *Saccharomyces cerevisiae*. *J Biol Chem* **266**, 20103–20109.
- Jacobs, N., Chen, R. A.-J., Gubser, C., Najjarro, P. & Smith, G. L. (2006).** Intradermal immune response after infection with vaccinia virus. *J Gen Virol* **87**, 1157–1161.
- Kettle, S., Alcami, A., Khanna, A., Ehret, R., Jassoy, C. & Smith, G. L. (1997).** Vaccinia virus serpin B13R (SPI-2) inhibits interleukin-1 β -converting enzyme and protects virus-infected cells from TNF- and Fas-mediated apoptosis, but does not prevent IL-1 β -induced fever. *J Gen Virol* **78**, 677–685.
- Kunstfeld, R., Lechleitner, S., Wolff, K. & Petzelbauer, P. (1998).** MCP-1 and MIP-1 α are most efficient in recruiting T cells into the skin *in vivo*. *J Invest Dermatol* **111**, 1040–1044.
- Macara, I. G. (2001).** Transport into and out of the nucleus. *Microbiol Mol Biol Rev* **65**, 570–594.
- Moss, B. (2001).** *Poxviridae: the viruses and their replication*. In *Virology*, 4th edn, pp. 2849–2883. Edited by B. N. Fields, D. M. Knipe, P. M. Howley, R. M. Chanock, J. Melnick, T. P. Monath, B. Roizman & S. E. Straus. Philadelphia: Lippincott-Raven Publishers.
- Niles, E. G. & Seto, J. (1988).** Vaccinia virus gene D8 encodes a virion transmembrane protein. *J Virol* **62**, 3772–3778.

Parkinson, J. E. & Smith, G. L. (1994). Vaccinia virus gene A36R encodes a M_r 43–50 K protein on the surface of extracellular enveloped virus. *Virology* **204**, 376–390.

Parkinson, J. E., Sanderson, C. M. & Smith, G. L. (1995). The vaccinia virus A38L gene product is a 33-kDa integral membrane glycoprotein. *Virology* **214**, 177–188.

Pires de Miranda, M., Reading, P. C., Tschärke, D. C., Murphy, B. J. & Smith, G. L. (2003). The vaccinia virus kelch-like protein C2L affects calcium-independent adhesion to the extracellular matrix and inflammation in a murine intradermal model. *J Gen Virol* **84**, 2459–2471.

Reading, P. C. & Smith, G. L. (2003). A kinetic analysis of immune mediators in the lungs of mice infected with vaccinia virus and comparison with intradermal infection. *J Gen Virol* **84**, 1973–1983.

Sanderson, C. M., Parkinson, J. E., Hollinshead, M. & Smith, G. L. (1996). Overexpression of the vaccinia virus A38L integral membrane protein promotes Ca^{2+} influx into infected cells. *J Virol* **70**, 905–914.

Schon, M. P., Zollner, T. M. & Boehncke, W. H. (2003). The molecular basis of lymphocyte recruitment to the skin: clues for pathogenesis and selective therapies of inflammatory disorders. *J Invest Dermatol* **121**, 951–962.

Seet, B. T., Johnston, J. B., Brunetti, C. R. & 7 other authors (2003). Poxviruses and immune evasion. *Annu Rev Immunol* **21**, 377–423.

Smith, G. L. & McFadden, G. (2002). Smallpox: anything to declare? *Nat Rev Immunol* **2**, 521–527.

Smith, G. L., Chan, Y. S. & Howard, S. T. (1991). Nucleotide sequence of 42 kbp of vaccinia virus strain WR from near the right inverted terminal repeat. *J Gen Virol* **72**, 1349–1376.

Smith, G. L., Vanderplasschen, A. & Law, M. (2002). The formation and function of extracellular enveloped vaccinia virus. *J Gen Virol* **83**, 2915–2931.

Spriggs, M. K., Hruby, D. E., Maliszewski, C. R., Pickup, D. J., Sims, J. E., Buller, R. M. & VanSlyke, J. (1992). Vaccinia and cowpox viruses encode a novel secreted interleukin-1-binding protein. *Cell* **71**, 145–152.

Tschärke, D. C. & Smith, G. L. (1999). A model for vaccinia virus pathogenesis and immunity based on intradermal injection of mouse ear pinnae. *J Gen Virol* **80**, 2751–2755.

Tschärke, D. C., Reading, P. C. & Smith, G. L. (2002). Dermal infection with vaccinia virus reveals roles for virus proteins not seen using other inoculation routes. *J Gen Virol* **83**, 1977–1986.

Upton, C., Slack, S., Hunter, A. L., Ehlers, A. & Roper, R. L. (2003). Poxvirus orthologous clusters: toward defining the minimum essential poxvirus genome. *J Virol* **77**, 7590–7600.

van Eijl, H., Hollinshead, M., Rodger, G., Zhang, W. H. & Smith, G. L. (2002). The vaccinia virus F12L protein is associated with intracellular enveloped virus particles and is required for their egress to the cell surface. *J Gen Virol* **83**, 195–207.

von Stebut, E., Metz, M., Milon, G., Knop, J. & Maurer, M. (2003). Early macrophage influx to sites of cutaneous granuloma formation is dependent on MIP-1 α/β released from neutrophils recruited by mast cell-derived TNF α . *Blood* **101**, 210–215.

Williamson, J. D., Reith, R. W., Jeffrey, L. J., Arrand, J. R. & Mackett, M. (1990). Biological characterization of recombinant vaccinia viruses in mice infected by the respiratory route. *J Gen Virol* **71**, 2761–2767.

Xu, L. & Massague, J. (2004). Nucleocytoplasmic shuttling of signal transducers. *Nat Rev Mol Cell Biol* **5**, 209–219.



Fig. 1. A rooted phylogenetic tree of VACV WR B14 and related poxvirus proteins. The sequences of the individual proteins were aligned using program clustal w and a rooted tree was derived from this alignment using phylip (phylogeny inference package, version 3.2) via Biology WorkBench 3.2 website (see <http://workbench.sdsc.edu/>). The bootstrap values from 1000 replica samplings are indicated. See www.poxvirus.org for details of B14 protein related proteins.

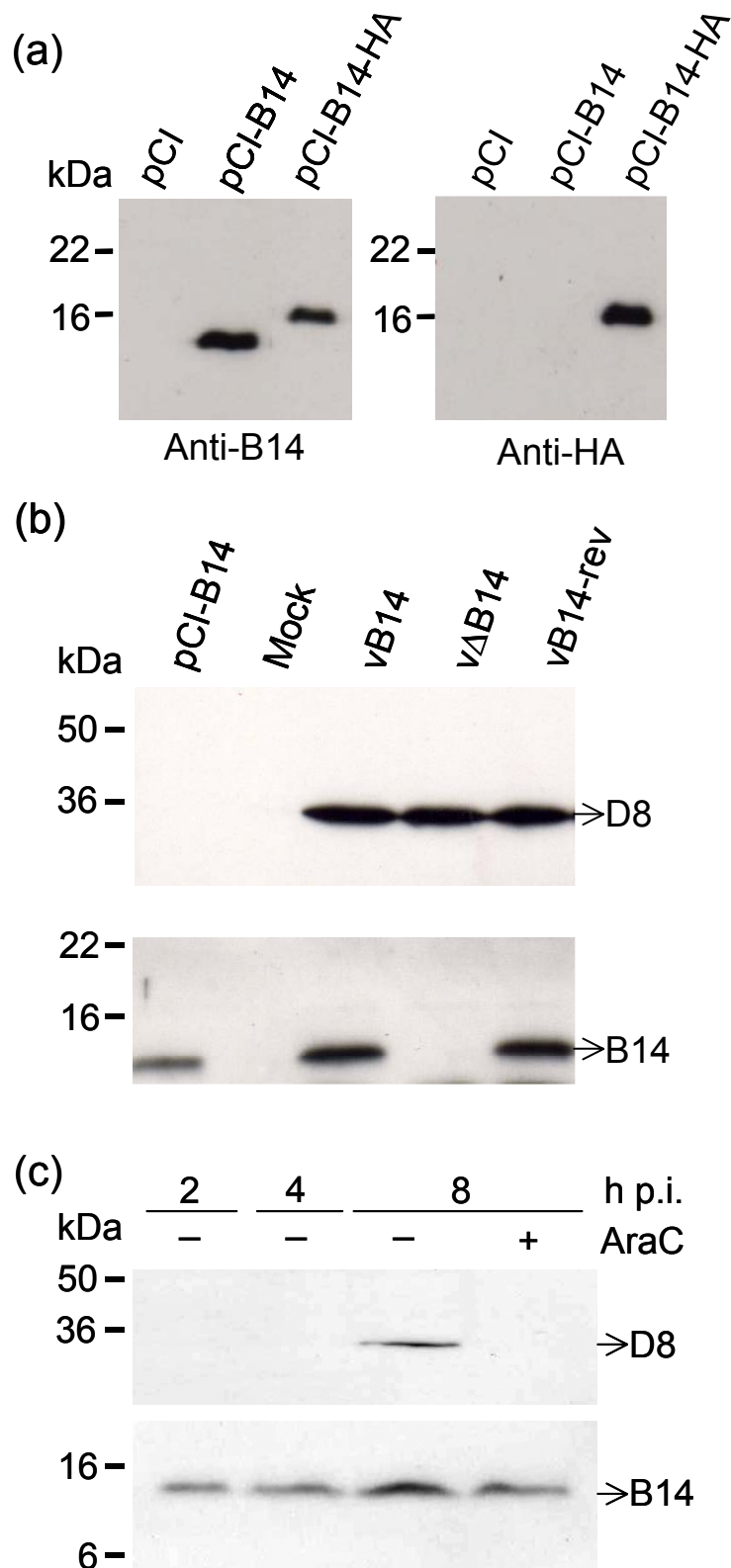


Fig. 2. Characterization of B14 by immunoblotting. (a) Wild-type and C-terminal HA-tagged B14 were expressed transiently in HeLa cells. At 24 h post-transfection, extracts of cells were prepared using RIPA buffer (20 mM Tris/HCl, pH 8.0, 150 mM NaCl, 1 % Nonidet P-40, 1 % SDS) and analysed by immunoblotting with either rabbit anti-B14 Ab (left) or an anti-HA mAb (right). (b) HeLa cells were infected by the indicated VACVs at 10 p.f.u. per cell for 16 h, or mock infected or transfected with pCI-B14 for 24 h. The cells were lysed in RIPA buffer and extracts were analysed by immunoblotting with anti-D8 mAb (top panel) or anti-B14 Ab (lower

panel). (c) HeLa cells were infected with VACV WR at 10 p.f.u. per cell in the presence (+) or absence (–) of 40 $\mu\text{g AraC ml}^{-1}$. At the indicated times p.i., the cells were washed once with PBS and lysed by addition of 200 μl protein loading buffer. Each cell lysate (20 μl) was resolved by SDS-PAGE and analysed by immunoblotting with anti-D8 mAb (top panel) or anti-B14 Ab (lower panel).

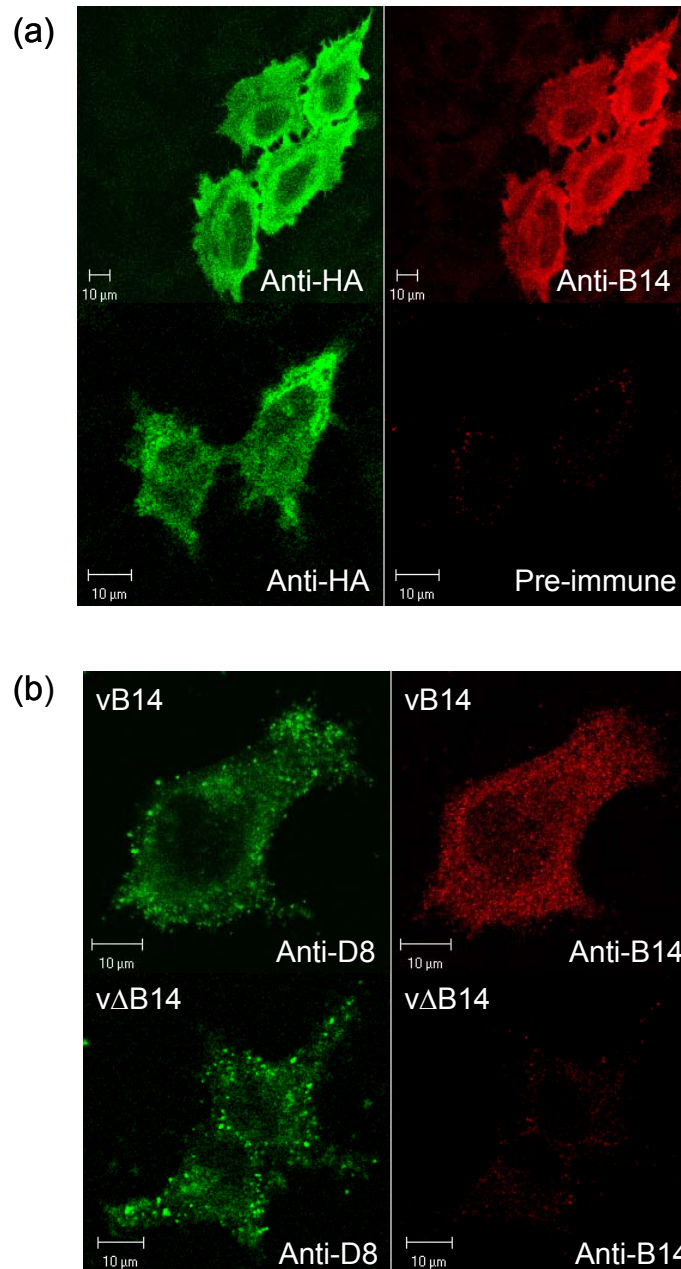


Fig. 3. Subcellular localization of B14. (a) B14 with a C-terminal HA tag was expressed transiently by transfection in HeLa cells for 24 h. Cells were fixed and permeabilized as described in Methods and stained with anti-HA mAb (left panels), anti-B14 Ab (top right panel) or rabbit pre-immune serum Abs (bottom right panel). (b) HeLa cells were infected with vB14 (top panels) or vΔB14 (lower panels) at 10 p.f.u. per cell for 8 h. Cells were fixed and permeabilized as in (a) and stained with either anti-D8 mAb (left panels) or anti-B14 Ab (right panels).

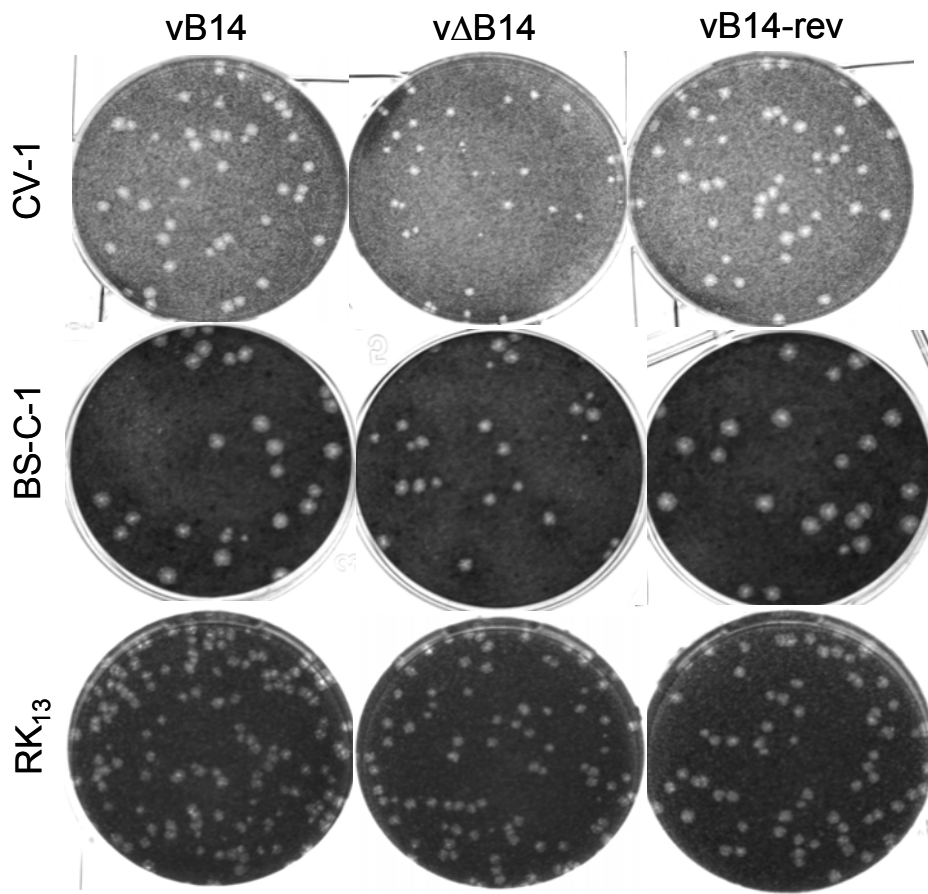


Fig. 4. Plaque formation by vΔB14. Monolayers of CV-1, RK₁₃ or BS-C-1 cells were infected by vB14, vΔB14 or vB14-rev and overlaid with DMEM/2.5 % FBS/1 % carboxymethyl cellulose. After 48 (CV-1 and BSC-1 cells) or 72 h (RK₁₃ cells), the monolayers were stained with 0.1 % crystal violet in 15 % ethanol and photographed.

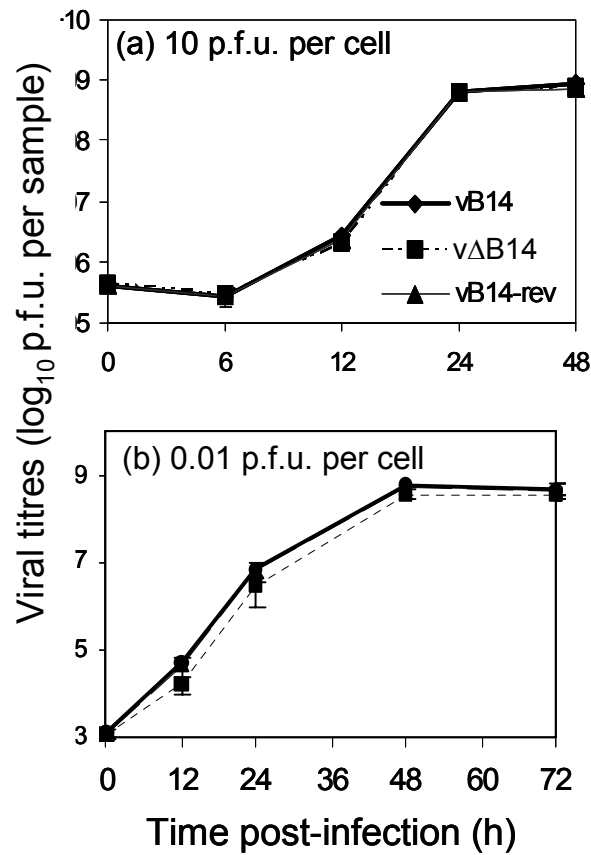
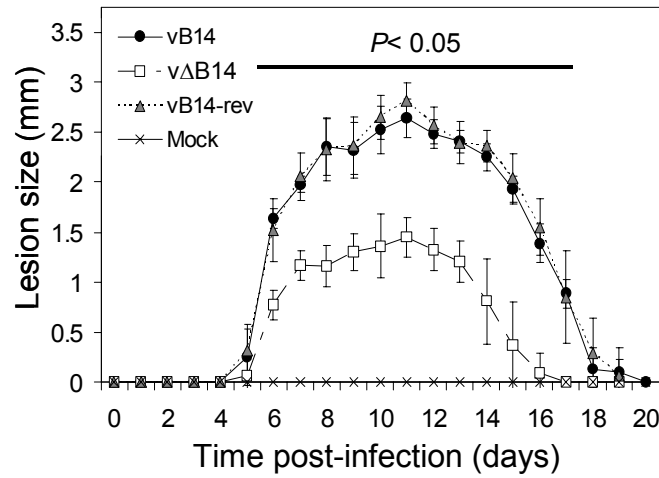


Fig. 5. Growth kinetics of vΔB14. BS-C-1 cells were infected at either 10 (a) or 0.01 (b) p.f.u. per cell and aliquots of infected cells were collected at the indicated times p.i. Cells were frozen and thawed three times, sonicated and the virus infectivity was titrated in duplicate on BS-C-1 cell monolayers. Data are presented as the mean log₁₀ p.f.u. ± SD.

(a)



(b)

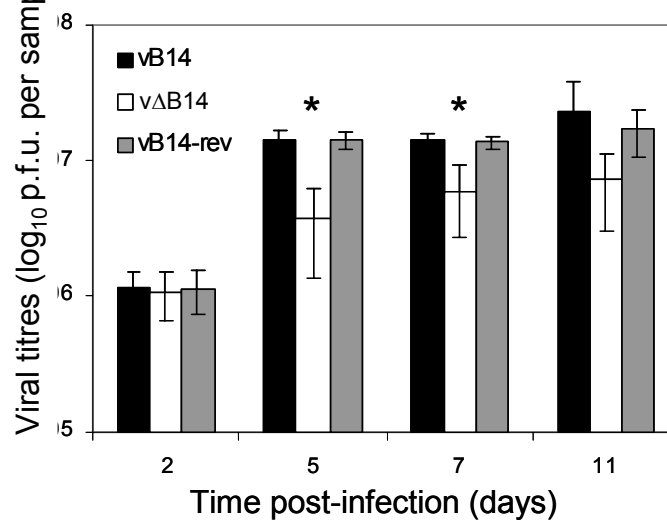


Fig. 6. Virulence assay in murine i.d. model. (a) Female C57BL/6 mice ($n=6$) were infected i.d. with 10^4 p.f.u. of the indicated viruses and the size of the lesion was measured daily with a micrometer. Horizontal bar indicates the days on which the lesion size caused by vΔB14 was statistically different ($P<0.05$) from both vB14 and vB14-rev. Data are means of lesion size \pm SD. (b) Infectious virus in infected lesions. Mice were infected in both ears as in (a) and at the indicated time p.i. the animals were sacrificed, ears were removed and infectious virus was determined by plaque assay on duplicate monolayers of BS-C-1 cells. Asterisks indicate days on which the titre of virus present in ears infected with vΔB14 was significantly different from both vB14 and vB14-rev-infected tissue. Data are means of viral titres \pm SD.

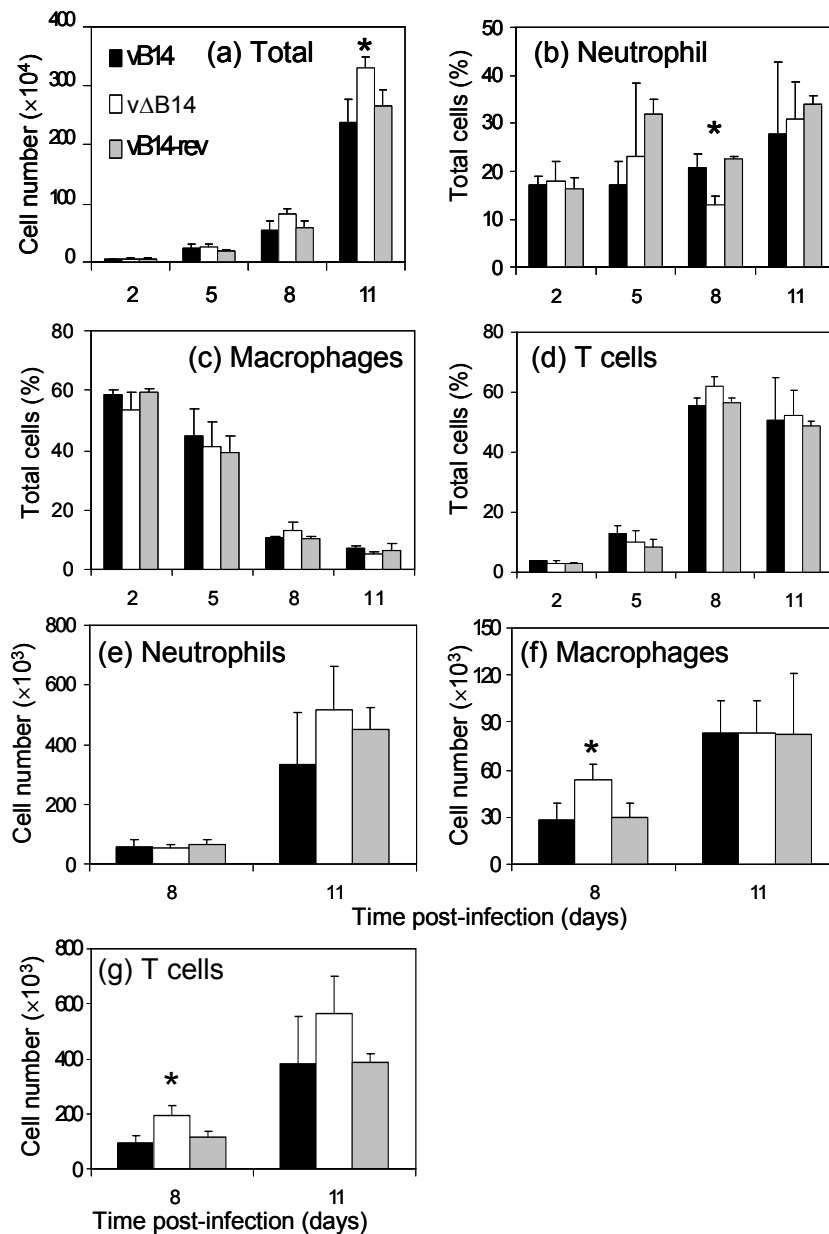


Fig. 7. Characterization of infiltrating leukocytes in the C57BL/6 mice infected intradermally with 10^4 p.f.u. of the indicated viruses. Cells were extracted (Methods) from both ears of an infected mouse and pooled. (a) Total numbers of viable cells were determined by trypan blue exclusion. Data are means of cell counts \pm SD. In these cells, neutrophils (b), macrophages (c) and T cells (d) were identified by corresponding surface markers as described in Methods. The absolute number of neutrophils (e), macrophages (f) and T cells (g) at days 8 and 11 p.i. were determined as described in Methods. The mean \pm SD of data from three infected mice were analysed. Asterisks indicate the day on which data for vΔB14 are significantly different from the vB14 and vB14-rev groups ($P < 0.05$, Student's *t*-test).